Deblurring Text Images via L_0-Regularized Intensity and Gradient Prior

Jinshan Pan†, Zhe Hu‡, Zhixun Su†, Ming-Hsuan Yang‡
† School of Mathematical Sciences, Dalian University of Technology
‡ Electrical Engineering and Computer Science, University of California at Merced
jspan@mail.dlut.edu.cn, zhu@ucmerced.edu, zxsu@dlut.edu.cn, mhyang@ucmerced.edu

Abstract

We propose a simple yet effective L_0-regularized prior based on intensity and gradient for text image deblurring. The proposed image prior is motivated by observing distinct properties of text images. Based on this prior, we develop an efficient optimization method to generate reliable intermediate results for kernel estimation. The proposed method does not require any complex filtering strategies to select salient edges which are critical to the state-of-the-art deblurring algorithms. We discuss the relationship with other deblurring algorithms based on edge selection and provide insight on how to select salient edges in a more principled way. In the final latent image restoration step, we develop a simple method to remove artifacts and render better deblurred images. Experimental results demonstrate that the proposed algorithm performs favorably against the state-of-the-art text image deblurring methods. In addition, we show that the proposed method can be effectively applied to deblur low-illumination images.

1. Introduction

The recent years have witnessed significant advances in single image deblurring [8]. Much success of the state-of-the-art algorithms [6, 16, 3, 18, 12, 10, 20] can be attributed to the use of learned prior from natural images and the selection of salient edges for kernel estimation. Although numerous methods [6, 16, 12, 10, 20] have been proposed for motion deblurring, these priors are less effective for text images due to the contents of interest being mainly two-toned (black and white) which do not follow the heavy-tailed gradient statistics of natural images.

Text image deblurring has attracted considerable attention in recent years due to its wide range of applications. In [1], Chen *et al*. propose a new prior based on the image intensity rather than the heavy-tailed gradient prior of natural scenes. However, this method is developed specifically for document images (*i.e*., binary text images) and is unlikely to work well for cluttered images with text. A direct method that exploits sparse characteristics of natural images is proposed for deblurring natural and document images [14]. Nevertheless, the blur kernel is not explicitly estimated from an input image and the computational load for learning an over-complete dictionary for deblurring is significant. Li and Lii [13] propose a joint estimation method to estimate blur kernels from two-tone images. However, this method is only applied to two-tone images and is less effective for text images with complex backgrounds. Cho *et al*. [2] develop a method to incorporate text-specific properties (*i.e*., sharp contrast between text and background, uniform gradient within text, and background gradient following natural image statistics) for deblurring. While this algorithm achieves the state-of-the-art deblurring results, the kernel estimation process is complicated and the performance depends largely on whether the stroke width transform (SWT) [5] separates an image into text and non-text regions well or not. If the characters in a text image are small and connected, it is unlikely to perform well. Figure 1 shows one example, where blurred characters are connected

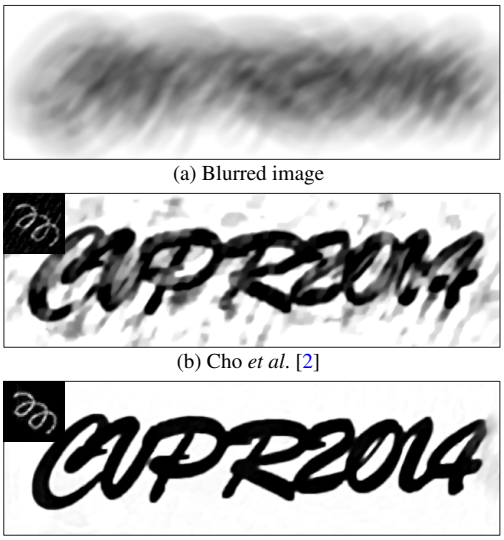

(a) Blurred image

(b) Cho *et al*. [2]

(c) Ours

Figure 1. A challenging blurred text image. (best viewed on high-resolution display).

due to large camera motion, and the deblurred result from the state-of-the-art algorithm [2].

In this paper, we propose a novel L_0-regularized intensity and gradient prior for text image deblurring, and present an efficient optimization algorithm based on the half-quadratic splitting method. The splitting method guarantees that each sub-problem has a closed-form solution and ensures fast convergence. We present analysis on the relationship with other methods based on salient edges, and show that the proposed algorithm generates reliable intermediate results for kernel estimation without any ad-hoc selection processes. Compared to the state-of-the-art methods [1, 2], the proposed algorithm is simple and easy to implement as it requires no additional operations (*e.g.*, adaptive segmentation [1], smoothing intermediate latent images, or SWT [2]). In the latent image restoration step, we present a simple method to deal with artifacts. Furthermore, we show that the proposed algorithm can also be applied to effectively process natural blurred images containing text and low illumination images which are not handled well by most state-of-the-art deblurring methods.

2. Text Deblurring via L_0-Regularized Prior

In this section, we present a novel L_0-regularized prior of intensity and gradient for text image deblurring.

2.1. L_0-Regularized Intensity and Gradient Prior

The proposed L_0 intensity and gradient prior is based on the observation that text characters and background regions usually have near uniform intensity values in clean images without blurs. Figure 2(b) illustrates that the pixel intensities of a clean text image (Figure 2(a)) center around two values and the distribution has two peaks (near 0 and 255). In other words, the pixel values of text images are very sparse if we only consider zero peaks. For a blurred text image, the histogram of pixel intensity is different from that of a clean image. Figure 2(e) shows the histogram of pixel intensity (from a blurred image in (d)) where it cannot be modeled well by narrow peaks. Most importantly, it does not contain the zero peak. Namely, the pixel values of blurred text images are more dense. This intensity property is generic for text images and used as one regularization term in our formulation. For an image x, we define

$$P_t(x) = \|x\|_0, \tag{1}$$

where $\|x\|_0$ counts the number of nonzero values of x. With this criterion on pixel intensity, clean and blurred images can be differentiated.

Gradient priors are widely used for image deblurring as they have been shown to be effective in suppressing artifacts. As the intensity values of a clean text image are close to two-tone, the pixel gradients are likely to have a few nonzero values. Figure 2(c) and (f) show the horizontal

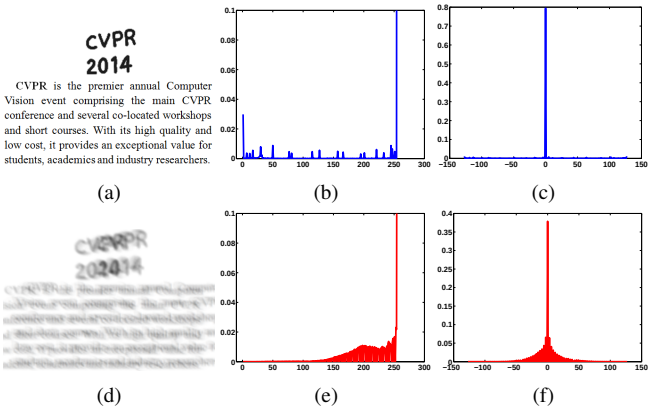

Figure 2. Statistics of text images. (a) clean text image. (b) histogram of pixel intensities from (a). (c) histogram of horizontal gradients from (a). (d) blurred image. (e) histogram of pixel intensities from (d). (f) histogram of horizontal gradients from (d).

gradient histograms of one clean text image and one blurred image. The nonzero values of blurred image gradients are denser than those of clear text image gradients. Thus we use L_0-regularized prior, $P_t(\nabla x)$, to model image gradients.

The image prior for text image deblurring is defined as

$$P(x) = \sigma P_t(x) + P_t(\nabla x), \tag{2}$$

where σ is a weight. Although $P(x)$ is developed based on the assumption that background regions of a text image are uniform, we show that this prior can also be applied to image deblurring with complex backgrounds.

2.2. Text Deblurring via L_0-Regularized Prior

The proposed prior $P(x)$ is used as a regularization term for text deblurring,

$$\min_{x,k} \|x * k - y\|_2^2 + \gamma\|k\|_2^2 + \lambda P(x), \tag{3}$$

where x and y denote the latent and blurred images, respectively; k is a blur kernel with the convolution operator * and L_2 regularized term $\|k\|_2^2$; and γ and λ are the weights.

3. Deblurring Text Images

We obtain the solution for (3) by alternatively solving

$$\min_{x} \|x * k - y\|_2^2 + \lambda P(x), \tag{4}$$

and

$$\min_{k} \|x * k - y\|_2^2 + \gamma\|k\|_2^2. \tag{5}$$

These two sub-problems are solved as follows.

3.1. Estimating x with k

Due to the L_0 regularization term in (4), minimizing (4) is commonly regarded as computationally intractable. Based on the half-quadratic splitting L_0 minimization method [19], we propose a new method to solve

it using an efficient alternating minimization method. We introduce auxiliary variables u and $g = (g_h, g_v)^\top$ corresponding to x and ∇x respectively, and rewrite the objective function as

$$\min_{x,u,g} \|x*k-y\|_2^2+\beta\|x-u\|_2^2+\mu\|\nabla x-g\|_2^2+\lambda(\sigma\|u\|_0+\|g\|_0), \tag{6}$$

where σ is the weight defined in (2). When β and μ are close to ∞, the solution of (6) approaches that of (4). With this formulation, (6) can be efficiently solved through alternatively minimizing x, u, and g independently by fixing the other variables.

The values of u and g are initialized to be zeros. In each iteration, the solution of x is obtained by solving

$$\min_x \|x * k - y\|_2^2 + \beta\|x - u\|_2^2 + \mu\|\nabla x - g\|_2^2, \tag{7}$$

and the closed-form solution for this least squares minimization problem is

$$x = \mathcal{F}^{-1}\left(\frac{\overline{\mathcal{F}(k)}\mathcal{F}(y) + \beta\mathcal{F}(u) + \mu F_G}{\overline{\mathcal{F}(k)}\mathcal{F}(k) + \beta + \mu\overline{\mathcal{F}(\nabla)}\mathcal{F}(\nabla)}\right), \tag{8}$$

where $\mathcal{F}(\cdot)$ and $\mathcal{F}^{-1}(\cdot)$ denote the Fast Fourier Transform (FFT) and inverse FFT, respectively; the $\overline{\mathcal{F}(\cdot)}$ is the complex conjugate operator; and $F_G = \overline{\mathcal{F}(\nabla_h)}\mathcal{F}(g_h) + \overline{\mathcal{F}(\nabla_v)}\mathcal{F}(g_v)$ where ∇_h and ∇_v denote the horizontal and vertical differential operators, respectively.

Given x, we compute u and g separately by

$$\begin{aligned} &\min_u \beta\|x - u\|_2^2 + \lambda\sigma\|u\|_0, \\ &\min_g \mu\|\nabla x - g\|_2^2 + \lambda\|g\|_0. \end{aligned} \tag{9}$$

Note that (9) is a pixel-wise minimization problem, thus, the solutions of u and g are obtained based on [19],

$$u = \begin{cases} x, & |x|^2 \geqslant \frac{\lambda\sigma}{\beta}, \\ 0, & \text{otherwise}, \end{cases} \tag{10}$$

and

$$g = \begin{cases} \nabla x, & |\nabla x|^2 \geqslant \frac{\lambda}{\mu}, \\ 0, & \text{otherwise}. \end{cases} \tag{11}$$

The main steps for solving (6) are summarized in Algorithm 1.

3.2. Estimating k with x

With the given x, (5) is a least squares minimization problem from which a closed-form solution can be computed by FFT. As the solution directly from (5) based on intensity values is not accurate [3, 12], we estimate the blur kernel k in the gradient space by

$$\min_k \|\nabla x * k - \nabla y\|_2^2 + \gamma\|k\|_2^2 \tag{12}$$

and the solution can be efficiently computed by FFTs [3].

Algorithm 1 Solving (6)

Input: Blur image y and blur kernel k.
$x \leftarrow y$, $\beta \leftarrow 2\lambda\sigma$.
repeat
  solve for u using (10).
  $\mu \leftarrow 2\lambda$.
  repeat
    solve for g using (11).
    solve for x using (8).
    $\mu \leftarrow 2\mu$.
  until $\mu > \mu_{\max}$
  $\beta \leftarrow 2\beta$.
until $\beta > \beta_{\max}$
Output: Intermediate latent image x.

Algorithm 2 Blur kernel estimation algorithm

Input: Blur image y.
initialize k with the results from the coarser level.
for $i = 1 \rightarrow 5$ **do**
  solve for x using Algorithm 1.
  solve for k using (12).
  $\lambda \leftarrow \max\{\lambda/1.1, 1e^{-4}\}$.
end for
Output: Blur kernel k and intermediate latent image x.

After obtaining k, we set the negative elements to 0, and normalize it so that the sum of its elements is 1.

Similar to the state-of-the-art methods, the proposed kernel estimation process is carried out in a coarse-to-fine manner using an image pyramid [3]. Algorithm 2 shows the main steps for kernel estimation algorithm on one pyramid level.

3.3. Removing Artifacts

Although latent text images can be estimated from (4) as shown in Figure 3(c), this formulation is less effective for scenes with complex backgrounds or fine texture details. We note that non-blind deblurring methods with Laplacian priors [9] have been shown to preserve fine details. However, significant artifacts are likely to be included with this prior as shown in Figure 3(b). In contrast, the proposed algorithm with L_0-regularized prior produces fewer fine details and ringing artifacts as shown in Figure 3(c).

The proposed algorithm can be further enhanced to deblur text and natural images with fine details by the following approach similar to the ringing suppression method [16]. First, we estimate latent images I_l (See Figure 3(b)) by using the method with Laplacian prior [9]. Second, we estimate latent images I_0 (See Figure 3(c)) using the proposed algorithm via (4) but only with the gradient information $P_t(\nabla x)$ at this stage (*i.e.*, setting σ of (6) to 0). Similar to [16], we then compute a difference map between these two estimated images and remove artifacts with bi-

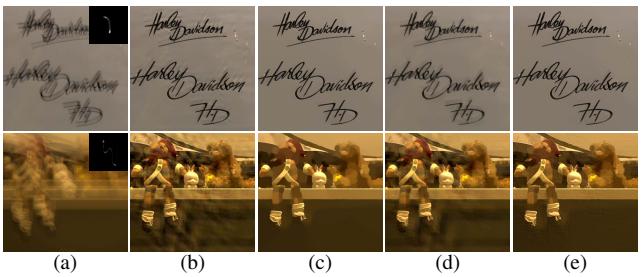

(a) (b) (c) (d) (e)

Figure 3. Non-blind deconvolution examples. (a) blurred images and our estimated kernels. (b) results by [9] with Laplacian prior. (c) results by (4) where $\sigma = 0$. (d) ringing suppression results by [16]. (e) our results.

lateral filtering. Finally, we subtract the filtered difference map from I_l. The result in Figure 3(e) shows that this approach works well for text and natural images, and performs favorably against the ringing suppression method [16].

4. Analysis of the Proposed Algorithm

In this section, we provide more insight and analysis on how the proposed algorithm performs on text deblurring. We also demonstrate the importance of intensity prior for text deblurring and discuss its relationship with other methods based on edge selection. Furthermore, we show that the proposed algorithm can be applied to deblur natural images.

4.1. Effectiveness of the L_0-Regularized Prior

The intensity prior $P_t(x)$ can be regarded as a regularization of segments based on image pixels from (10). In the proposed algorithm, the threshold value of (10) is decreasing with the effect of selecting segments in a coarse-to-fine manner. We note (10) is the critical step adopted in [1] for text deblurring.

The text deblurring method [2] has a similar step ((7) in [2]) to the sub-problem of u in (9). The main difference is that the threshold value in [2] is determined by SWT [5]. In addition, this text deblurring algorithm uses the sparse gradient minimization method [19] to remove ringing artifacts from the intermediate latent images, and thus has more computational loads. The effectiveness of this method is limited by SWT in terms of speed and accuracy. Figure 4 shows one example for which the method [2] does not perform well. The reason is that SWT is not effective in detecting text when the blurred characters are connected. The images in Figure 4(e) show the intermediate results generated by SWT in [2].

The success of recent deblurring methods hinges on intermediate estimations of the latent image explicitly [3, 18] or implicitly [6, 16, 10]. The proposed method is distinguished from existing methods as it does not involve ad-hoc edge selection (*e.g.*, spatial filtering [2, 3, 18], or edge reweighting [16, 10]) for kernel estimation. Instead of finding one good threshold to remove subtle image structures

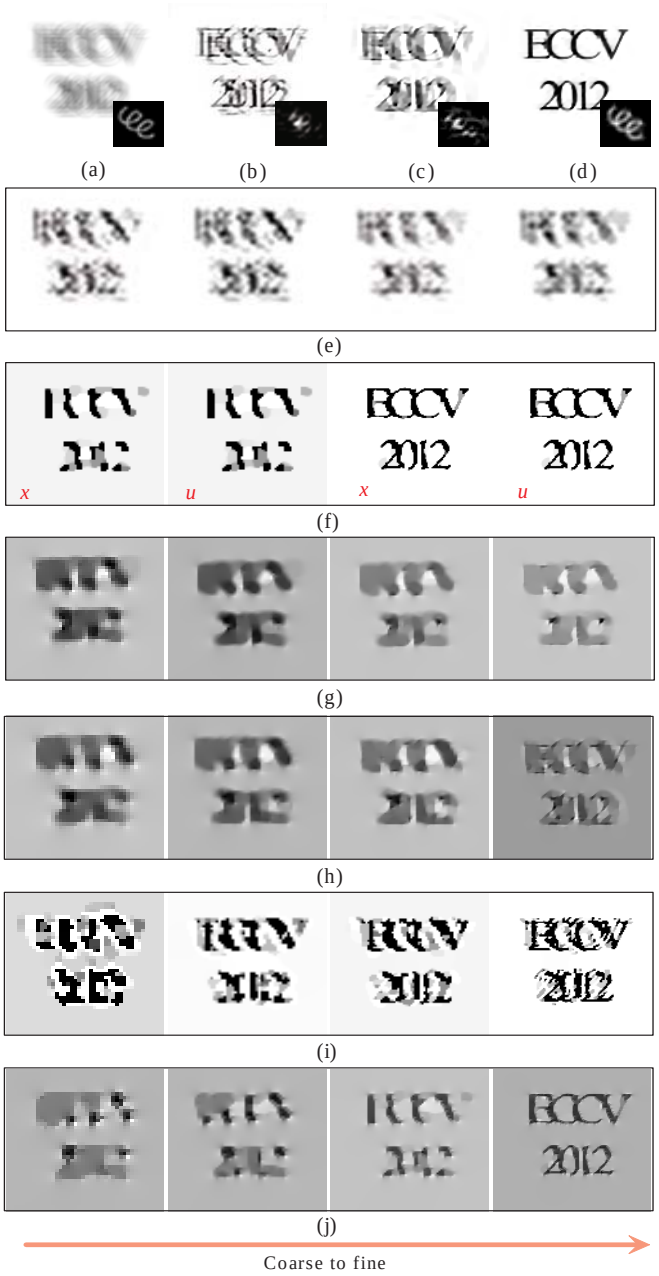

Figure 4. An example presented in [2]. (a) blurred image and kernel. (b) results of [2]. (c) our results without using $P_t(x)$ in the kernel estimation. (d) our final results. (e) intermediate results of [2]. (f) our intermediate results (including x and u). (g) intermediate salient edges of [20]. (h) intermediate salient edges using only $P_t(\nabla x)$. (i) intermediate results using only $P_t(x)$. (j) our intermediate salient edges, *i.e.*, g in (11).

like the filter-based edge selection methods [3, 18], the proposed algorithm computes intermediate estimations iteratively by solving a few optimization problems in a way similar to [20]. By using (10) and (11) in the proposed algorithm, pixels with small intensity values or tiny structures can be removed while salient edges are retained. Further-

more, our method exploits the gradient prior with $P_t(\nabla x)$. If σ of (6) is set to 0, then the proposed algorithm is similar to the recent methods based on L_0 gradient priors [20, 15] which achieve the state-of-the-art results for deblurring natural images. Thus, the proposed algorithm is likely to perform well for natural image deblurring. On the other hand, these two methods [20, 15] (L0Deblur for short) do not perform well for text images. Figure 4(g) shows intermediate salient edges extracted by [20]. As no sharp edges are extracted, the blur kernel is not estimated well by this method.

We note that image deblurring using only intensity prior $P_t(x)$ is less effective (See Figure 4(i)) as the intensity prior does not guarantee the sparsity properties of text image gradients. On the other hand, image deblurring with only gradient prior $P_t(\nabla x)$ is not effective (See Figure 4(h)) as no salient edges are extracted.

4.2. Convergence of the Proposed Algorithm

Our kernel estimation algorithm is mainly based on the alternating minimization method which ensures that each sub-problem has a closed-form solution. Thus, it has the fast convergence property. Figure 5(c) shows kernel similarity [7] with respect to iterations. With more iterations, the quality of kernel estimates becomes higher.

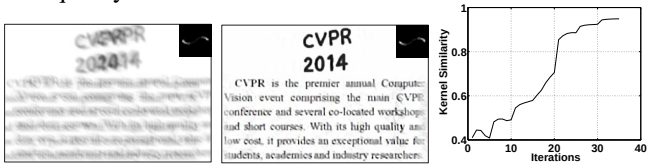

(a) Input and kernel (b) Our results (c) Kernel similarity plot

Figure 5. Convergence of the proposed algorithm.

4.3. Deblurring Non-document Text Images

Although the prior $P(x)$ is developed based on the assumptions that text images have uniform backgrounds, the proposed method can be applied to text deblurring in non-document text images as shown in Figure 6.

(a) Blurred image (b) Intermediate result x (c) Our results

Figure 6. An example with complex background regions. The size of estimated kernel is 99×99 pixels.

In the proposed Algorithm 1, the solution u from (10) contains large intensity values and g from (11) contains large gradient values. That is, u and g contain main structures of x. Thus, the intermediate result from (7) is likely to inherit the properties of u and g. Compared to the natural image deblurring method [20], our intermediate latent image restoration step introduces the intensity prior $P_t(x)$. This prior can help preserve more salient edges in the intermediate latent image rather than destroy the salient edges (*e.g.*, Figure 4(j)). Figure 6(b) shows an intermediate latent image x from a natural image. The result demonstrates that the use of prior $P(x)$ can also preserve salient edges and removes tiny details in natural images, thereby facilitating kernel estimation in natural images.

4.4. Deblurring Saturated Images

Estimating motion kernels from blurred images with regions of saturated pixels has been known as a difficult problem. Although some non-blind deblurring methods [4, 17] have been proposed, it remains challenging to develop effective blind deblurring algorithms. Saturated regions usually appear sparsely in clear images and these areas are much larger (*e.g.*, blobs or streaks) in the blurred images. Figure 7(b) shows two examples of saturated images from Figure 7(a). As the L_0 norm used in the proposed algorithm is similar to an adaptive hard threshold strategy, we use the binary images for illustration. Figure 7(c) and (d) show the corresponding binary images of clear and blurred saturated images where there are more nonzero elements in the blurred binary images than those in the clear binary images. As the L_0 norm in $P_t(x)$ minimizes the number of nonzero coefficients, the proposed deblurring algorithm favors solutions with fewer blobs or streaks in the latent clear images. We present results from challenging examples in Section 5.2.

(a) (b) (c) (d)

Figure 7. Saturated images. (a) Clear images with saturated areas and kernel. (b) Blurred images with saturated areas. (c) Binary images of (a). (d) Binary images of (b). (c) and (d) are obtained from (a) and (b) with the same threshold value.

5. Experimental results

We present experimental evaluations of the proposed algorithm against the state-of-the-art methods for text deblurring and results for saturated images in this section. All the experiments are carried out on a desktop computer with an Intel Xeon processor and 12 GB RAM. The execution time for a 255×255 image is around 50 seconds on MATLAB. In all the experiments, we set $\lambda = 4e^{-3}$, $\gamma = 2$, and $\sigma = 1$, respectively. We empirically set $\beta_{\max} = 2^3$ and $\mu_{\max} = 1e^5$ in Algorithm 1. More experimental results can be found in the supplementary document, and the MATLAB code and datasets are available at http://eng.ucmerced.edu/people/zhu/cvpr14_textdeblur.

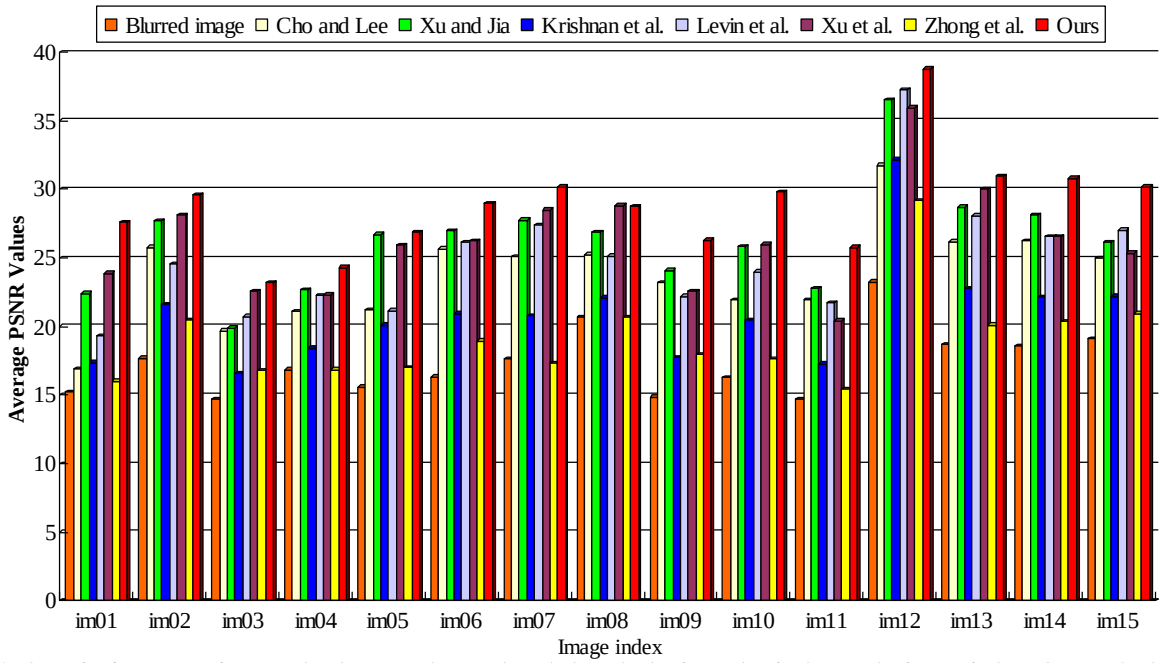

Figure 8. Quantitative comparison on the dataset. The numbers below the horizontal axis denote the image index. Our method performs the best.

5.1. Document Images

Synthetic images: We provide the example from [2] as shown in Figure 4 for comparison. Table 1 shows the SSIM values and the kernel similarity values of the recovered images and estimated kernels by some state-of-the-art methods. Overall, the proposed algorithm performs well in terms of both metrics. In addition, we build a dataset containing 15 ground truth document images and 8 kernels from [11]. For each sharp image, we compute the average PSNR on the blurred images from different kernels and compare among different methods [16, 3, 18, 10, 12, 20, 21] in Figure 8. The details about this dataset can be found in the supplementary document.

Real images: We evaluate the proposed algorithm and other methods using real images. For fair comparison with [2], we use an example from [2] and show the deblurred results in Figure 9. The natural image deblurring methods do not perform well on text images. The deblurred result of [1] contains some ringing artifacts and some details are missing. Although the state-of-the-art method by Cho *et al*. [2] performs well, the motion blur is not fully removed as shown in the red box in Figure 9(g). In addition, the deblurred results contain unnatural colors as a result of the SWT process. Compared with [2], the proposed algorithm generates a sharper and visually more pleasant deblurred image. We note that the L0Deblur [20] does not estimate the blur kernel or deblurs the image well which also demonstrates the importance of $P_t(x)$ of the proposed prior $P(x)$.

5.2. Non-document Images

Non-document text images: We present an example in Figure 10 where the complex image contains rich text and cluttered background regions. The state-of-the-art natural image deblurring methods [3, 18, 21, 20, 6] do not perform well in this image. Although the text deblurring method [2] handles this image well, the estimated kernel contains a certain amount of noise and the deblurred result contains some unnatural colors as a result of the SWT process. In contrast, the proposed algorithm generates the deblurred image (clear text, sharp edges, and natural color) and blur kernel well. Figure 10(h) and (i) show the results using the proposed algorithm without $P_t(x)$ and $P_t(\nabla x)$, respectively. The results in (h)-(i) show that sharp images cannot be obtained by using only the gradient prior or intensity prior, which indicates that the proposed prior $P(x)$ plays a critical role in text image deblurring.

Low-illumination images: It is known that most state-of-the-art deblurring methods are less effective in processing blurred images with saturated regions [4] which often appear in low-illumination scenes. As discussed in Section 4.4, the proposed algorithm is likely to handle this problem to a certain extent.

Figure 11 shows a real captured image which contains several saturated regions (red boxes in (a)). We compare the proposed algorithm with the state-of-the-art methods [3, 18, 10, 21, 20]. As the priors of the state-of-the-art methods are developed to exploit salient edges for motion

Table 1. Quantitative comparison using the example shown in Figure 4(a).

	[3]	[18]	[12]	[20]	[21]	[2]	Ours without $P_t(x)$	Ours without $P_t(\nabla x)$	Ours
SSIM of images	0.6457	0.6269	0.5611	0.4867	0.6190	0.5526	0.5812	0.7473	**0.8659**
Kernel similarity	0.5200	0.5200	0.4170	0.6407	0.4938	0.6456	0.6303	0.7133	**0.9140**

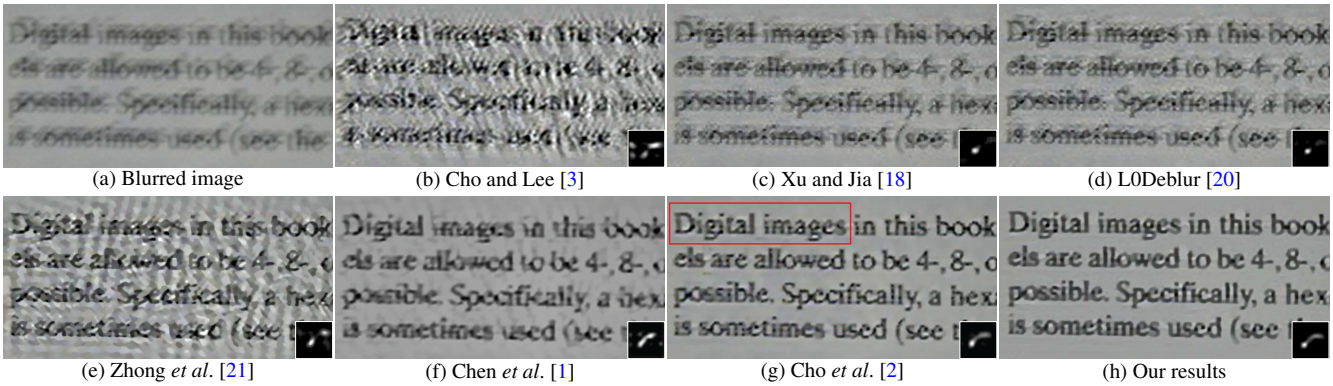

(a) Blurred image (b) Cho and Lee [3] (c) Xu and Jia [18] (d) L0Deblur [20]

(e) Zhong *et al*. [21] (f) Chen *et al*. [1] (g) Cho *et al*. [2] (h) Our results

Figure 9. A real blurred image from [2]. The part in the red box in (g) contains some blur and unnatural colors.

deblurring, these algorithms do not perform well for images containing numerous saturated regions. While the recent method [21] is developed to handle large Gaussian noise, it is less effective for saturated images. Although the saturated areas (*e.g*., the highlighted blobs, streaks, and the characters in Figure 11(a)) are large due to motion blur, as discussed in Section 4.4, the L_0-regularized prior $P(x)$ favors a clean image with few blobs and streaks. Thus, the proposed algorithm is able to estimate the blur kernel well due to the proposed prior $P(x)$. The recovered image shown in Figure 11(g) is sharper and clearer and characters can be recognized. We note that while our method is able to estimate the blur kernel well, there still exist some ringing artifacts due to the limitation of the final latent image estimation process (Figure 11(g)). To generate better deblurred results, we employ the non-blind deconvolution method [17]. The deblurred results shown in Figure 11(h) contain clearer text information and finer textures which demonstrates the effectiveness of the proposed algorithm for kernel estimation.

6. Conclusion

In this paper, we propose a simple yet effective prior for text image deblurring. While the proposed prior is based on the properties of two-tone text images, it can also be effectively applied to non-document text images and low-illumination scenes with saturated regions. With this prior, we present an effective optimization method based on a half-quadratic splitting strategy, which ensures that each sub-problem has a closed-form solution. The proposed method does not require any complex processing techniques, *e.g*., filtering, adaptive segmentation or SWT. In addition, we develop a simple latent image restoration method which helps reduce artifacts effectively. Our future work will focus on a better non-blind deconvolution method and extend the proposed algorithm to non-uniform text image deblurring.

Acknowledgements We thank Hojin Cho for generating the deblurred results of his method [2]. Jinshan Pan and Zhixun Su are supported by the NSFC (Nos. 61300086, 61173103 and 91230103), the China Postdoctoral Science Foundation, and National Science and Technology Major Project (2013ZX04005021). Zhe Hu and Ming-Hsuan Yang are supported partly by the NSF CAREER Grant (No. 1149783) and NSF IIS Grant (No. 1152576).

References

[1] X. Chen, X. He, J. Yang, and Q. Wu. An effective document image deblurring algorithm. In *CVPR*, pages 369–376, 2011. 1, 2, 4, 6, 7

[2] H. Cho, J. Wang, and S. Lee. Text image deblurring using text-specific properties. In *ECCV*, pages 524–537, 2012. 1, 2, 4, 6, 7, 8

[3] S. Cho and S. Lee. Fast motion deblurring. *ACM Trans. Graph.*, 28(5):145, 2009. 1, 3, 4, 6, 7, 8

[4] S. Cho, J. Wang, and S. Lee. Handling outliers in non-blind image deconvolution. In *ICCV*, pages 495–502, 2011. 5, 6

[5] B. Epshtein, E. Ofek, and Y. Wexler. Detecting text in natural scenes with stroke width transform. In *CVPR*, pages 2963–2970, 2010. 1, 4

[6] R. Fergus, B. Singh, A. Hertzmann, S. T. Roweis, and W. T. Freeman. Removing camera shake from a single photograph. *ACM Trans. Graph.*, 25(3):787–794, 2006. 1, 4, 6

[7] Z. Hu and M.-H. Yang. Good regions to deblur. In *ECCV*, pages 59–72, 2012. 5

[8] R. Köhler, M. Hirsch, B. J. Mohler, B. Schölkopf, and S. Harmeling. Recording and playback of camera shake: Benchmarking blind deconvolution with a real-world database. In *ECCV*, pages 27–40, 2012. 1

[9] D. Krishnan and R. Fergus. Fast image deconvolution using Hyper-Laplacian priors. In *NIPS*, pages 1033–1041, 2009. 3, 4

[10] D. Krishnan, T. Tay, and R. Fergus. Blind deconvolution using a normalized sparsity measure. In *CVPR*, pages 2657–2664, 2011. 1, 4, 6, 8

[11] A. Levin, Y. Weiss, F. Durand, and W. T. Freeman. Understanding and evaluating blind deconvolution algorithms. In *CVPR*, pages 1964–1971, 2009. 6

[12] A. Levin, Y. Weiss, F. Durand, and W. T. Freeman. Efficient marginal likelihood optimization in blind deconvolution. In *CVPR*, pages 2657–2664, 2011. 1, 3, 6, 7

[13] T.-H. Li and K.-S. Lii. A joint estimation approach for two-tone image deblurring by blind deconvolution. *IEEE Transactions on Image Processing*, 11(8):847–858, 2002. 1

(a) Blurred image (b) Cho and Lee [3] (c) Xu and Jia [18] (d) Krishnan *et al*. [10] (e) L0Deblur [20]

(f) Zhong *et al*. [21] (g) Cho *et al*. [2] (h) Ours without $P_t(x)$ (i) Ours without $P_t(\nabla x)$ (j) Our results

Figure 10. A blurred image with rich text. Our method performs well at kernel estimation and image recovery.

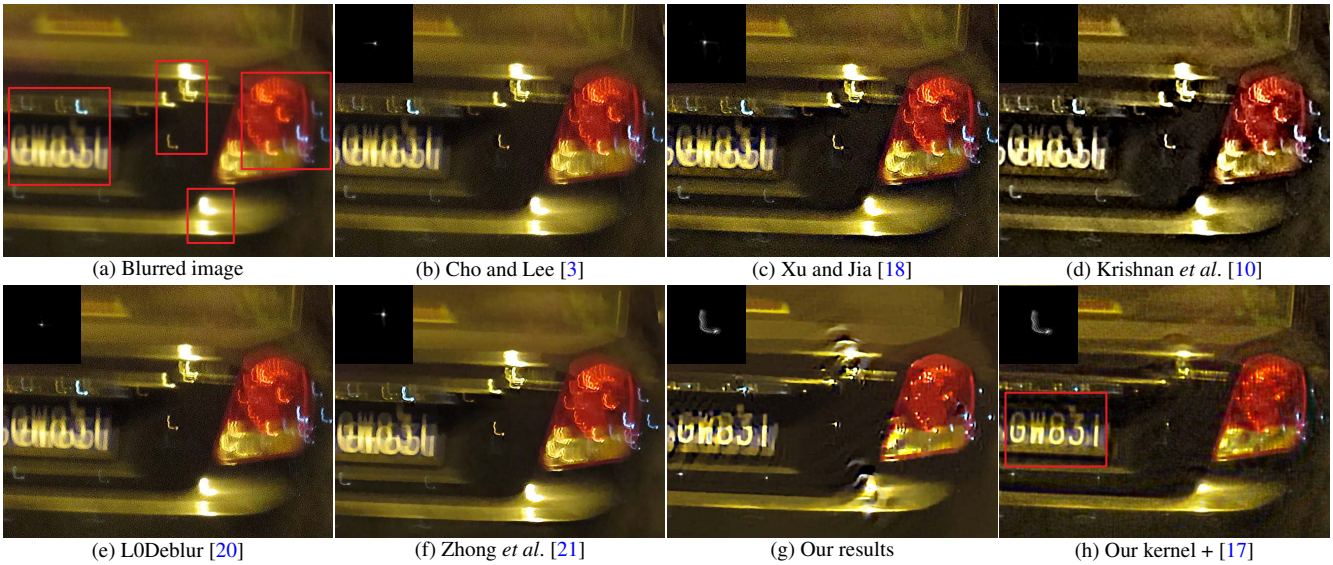

(a) Blurred image (b) Cho and Lee [3] (c) Xu and Jia [18] (d) Krishnan *et al*. [10]

(e) L0Deblur [20] (f) Zhong *et al*. [21] (g) Our results (h) Our kernel + [17]

Figure 11. A real blurred image with numerous saturated regions. The red boxes in (a) enclose some saturated pixels (*e.g*., the highlighted blobs, streaks, and the characters).

[14] Y. Lou, A. L. Bertozzi, and S. Soatto. Direct sparse deblurring. *Journal of Mathematical Imaging and Vision*, 39(1):1–12, 2011. 1

[15] J. Pan and Z. Su. Fast ℓ^0-regularized kernel estimation for robust motion deblurring. *IEEE Signal Processing Letters*, 20(9):841–844, 2013. 5

[16] Q. Shan, J. Jia, and A. Agarwala. High-quality motion deblurring from a single image. *ACM Trans. Graph.*, 27(3):73, 2008. 1, 3, 4, 6

[17] O. Whyte, J. Sivic, and A. Zisserman. Deblurring shaken and partially saturated images. In *ICCV Workshops*, pages 745–752, 2011. 5, 7, 8

[18] L. Xu and J. Jia. Two-phase kernel estimation for robust motion deblurring. In *ECCV*, pages 157–170, 2010. 1, 4, 6, 7, 8

[19] L. Xu, C. Lu, Y. Xu, and J. Jia. Image smoothing via l_0 gradient minimization. *ACM Trans. Graph.*, 30(6):174, 2011. 2, 3, 4

[20] L. Xu, S. Zheng, and J. Jia. Unnatural l_0 sparse representation for natural image deblurring. In *CVPR*, pages 1107–1114, 2013. 1, 4, 5, 6, 7, 8

[21] L. Zhong, S. Cho, D. Metaxas, S. Paris, and J. Wang. Handling noise in single image deblurring using directional filters. In *CVPR*, pages 612–619, 2013. 6, 7, 8